Hard-sphere fluid adsorbed in an annular wedge: The depletion force of hard-body colloidal physics

A. R. Herring and J. R. Henderson
School of Physics and Astronomy, University of Leeds, Leeds LS2 9JT, United Kingdom
(Received 18 October 2006; published 5 January 2007)

Many important issues of colloidal physics can be expressed in the context of inhomogeneous fluid phenomena. When two large colloids approach one another in solvent, they interact at least partly by the response of the solvent to finding itself adsorbed in the annular wedge formed between the two colloids. At shortest range, this fluid mediated interaction is known as the depletion force/interaction because solvent is squeezed out of the wedge when the colloids approach closer than the diameter of a solvent molecule. An equivalent situation arises when a single colloid approaches a substrate/wall. Accurate treatment of this interaction is essential for any theory developed to model the phase diagrams of homogeneous and inhomogeneous colloidal systems. The aim of our paper is a test of whether or not we possess sufficient knowledge of statistical mechanics that can be trusted when applied to systems of large size asymmetry and the depletion force in particular. When the colloid particles are much larger than a solvent diameter, the depletion force is dominated by the effective two-body interaction experienced by a pair of solvated colloids. This low concentration limit of the depletion force has therefore received considerable attention. One route, which can be rigorously based on statistical mechanical sum rules, leads to an analytic result for the depletion force when evaluated by a key theoretical tool of colloidal science known as the Derjaguin approximation. A rival approach has been based on the assumption that modern density functional theories (DFT) can be trusted for systems of large size asymmetry. Unfortunately, these two theoretical predictions differ qualitatively for hard sphere models, as soon as the solvent density is higher than about 2/3 that at freezing. Recent theoretical attempts to understand this dramatic disagreement have led to the proposal that the Derjaguin and DFT routes represent opposite limiting behavior, for very large size asymmetry and molecular sized mixtures, respectively. This proposal implies that nanocolloidal systems lie in between the two limits, so that the depletion force no longer scales linearly with the colloid radius. That is, by decreasing the size ratio from mesoscopic to molecular sized solutes, one moves smoothly between the Derjaguin and the DFT predictions for the depletion force scaled by the colloid radius. We describe the results of a simulation study designed specifically as a test of compatibility with this complex scenario. Grand canonical simulation procedures applied to hard-sphere fluid adsorbed in a series of annular wedges, representing the depletion regime of hard-body colloidal physics, confirm that neither the Derjaguin approximation, nor advanced formulations of DFT, apply at moderate to high solvent density when the geometry is appropriate to nanosized colloids. Our simulations also allow us to report structural characteristics of hard-body solvent adsorbed in hard annular wedges. Both these aspects are key ingredients in the proposal that unifies the disparate predictions, via the introduction of new physics. Our data are consistent with this proposed physics, although as yet limited to a single colloidal size asymmetry.

DOI: 10.1103/PhysRevE.75.011402 PACS number(s): 82.70.Dd, 61.20.Gy, 68.03.Cd

I. INTRODUCTION

Equilibrium statistical mechanics of bulk and inhomogeneous liquids, applied to physicists models of molecular fluids, is today a mature and apparently well-understood branch of physics [1]. Recent attention has turned to colloidal systems, where the important issues boil down to whether or not methods developed for molecular models remain valid when one or more of the species is much larger than the solvent species. This size asymmetry leads naturally to descriptions based on inhomogeneous fluid phenomena. Colloidal systems have been intensively studied experimentally for almost a century, due to their technological significance. Probably the most important additional physics that arises because of a large size ratio between solute and solvent is the "depletion effect," which can be usefully discussed purely in terms of entropic (free volume and free surface area) contributions to the free energy [2–5]. Depletion dominates solute-solute and solute-wall interactions mediated by solvent, in the short-range regime where solvent molecules are excluded from the center of the annular wedge formed by the two solutes, or the solute and the wall, because of the finite size of the solvent particles.

In a recent letter [6], associated with this paper, we have presented the main conclusion of a simulation test of current understanding of hard-body colloidal physics. Earlier work had raised serious doubts as to whether or not widely used current statistical mechanical methods are applicable to model colloidal systems. The presence of a disparate size ratio between solute and solvent has a dramatic effect on the solvent mediated interaction between hard-body solutes in hard-sphere solvent, at least when one applies the ubiquitous theoretical tool of colloidal science known as the "Derjaguin approximation" [7]. At sufficiently close range where the colloid surfaces exclude solvent particles from penetrating between them, the "depletion regime," this class of statistical mechanical analysis predicts a linear solvent-mediated force, where the associated potential is attractive at low solvent

density but becomes repulsive at intermediate and high density. This physics is in total contradiction with the most sophisticated class of classical density functional theory, known as fundamental-measure-theory density functional theory (FMT-DFT) which is based on incorporating the geometric measures of hard-sphere geometry, at least when FMT-DFT is applied to a homogeneous colloidal mixture in the limit of low colloid concentration to obtain the dependence of the pair depletion force on solvent density [8,9]. The implications for a breakdown in either of these approaches represent a serious failure in current understanding of statistical mechanics applied to colloidal physics. Theoretical modeling of this qualitative disagreement/breakdown has implied that one should focus on the structure and statistical thermodynamics of the inhomogeneous solvent adsorbed within the annular wedge that is formed by an interacting pair of colloids or, alternatively, between a solute and a planar hard wall [10,11]. At the heart of the matter lies the significance, or otherwise, of a nearly planar-pore central region that arises when the two solutes are close to one solvent diameter apart. This can be interpreted as a contribution to the line tension that varies strongly with the separation of the colloids that is ignored by the Derjaguin approximation applied to this geometry. A quantitative estimation of the significance of this additional physics by Oettel [11] implies that it is grossly overestimated by FMT-DFT in even the nanocolloidal regime, while on the other hand the Derjaguin approximation is only correct in the mesoscopic colloidal limit. Thus the two rival statistical mechanical approaches seem to be valid only in opposite extremes, with the nanocolloidal world lying inevitably in between. This, in turn, implies a breakdown in the linear scaling of the solvation force with colloid radius, predicted by both FMT-DFT and the Derjaguin analysis. Below, we report the full details of a simulation test that strongly supports this complex scenario, based on direct measurement of the fluid mediated force within a series of systems consisting of hard-sphere solvent adsorbed within annular wedges, spanning the depletion regime. Section II explains the simulation procedures and the underlying statistical mechanics used to extract the depletion force from the measured density profile. In Sec. III we describe the structure of the adsorbed fluid and associated fluctuations and report the quasi-two-dimensional adsorption deep within the central region of the annular wedge. Section IV presents our results for the depletion force at a colloid-solvent size ratio of 20. For completeness, we re-present our high pressure data reported earlier [6], where the presence of new physics is unmistakable, but now compared with results at a lower solvent density that has been extensively studied before with DFT [8] simulation [12–14] and integral equation theories [12,13]. Finally, Sec. V critically discusses our main conclusions and notes implications for the future development of colloidal physics.

II. SIMULATION PROCEDURES AND ASSOCIATED STATISTICAL MECHANICS

Figure 1 is a scale drawing of the annular geometry of our simulation system. A hard spherical colloid of radius R is fixed at the origin, lying equidistant between a pair of planar hard walls lying parallel to the xy plane. The separation $2(R+h)$ of the walls is chosen to fix the closest approach of the walls to the colloid surface to be somewhere in the depletion regime $0 \leqslant h \leqslant \sigma$; where σ denotes the solvent hard-sphere diameter. Hard-sphere solvent is used for direct comparison with FMT-DFT. The dashed boundaries in Fig. 1 define the volume $V(h)$ and the surface area $A(h)$ accessible to solvent. That is, the center of a solvent sphere can approach no closer than $\sigma/2$ from either the planar walls or the colloid surface/wall. Thus the effective radius of curvature of the two annular wedges, defined by the above geometry, is $R'=R+\sigma/2$. The depletion volume and the associated loss of surface area can be identified in Fig. 1 as the region of overlap between the dashed boundaries. This overlap is a maximum at $h=0$ and reduces smoothly to zero as $h \to \sigma$. The annular radius of closest approach of a solvent center is

$$y_0 = \sqrt{2R'(\sigma-h)-(\sigma-h)^2} \simeq \sqrt{2R'(\sigma-h)}, \qquad (1)$$

which can be regarded as inducing a line-tension contribution to the free energy of the solvent. The essence of the Derjaguin approximation for the depletion force is that this line tension contribution is assumed to be independent of h throughout the depletion regime [10]. The annular radius y_b denotes a distance from the center of the wedge at which the

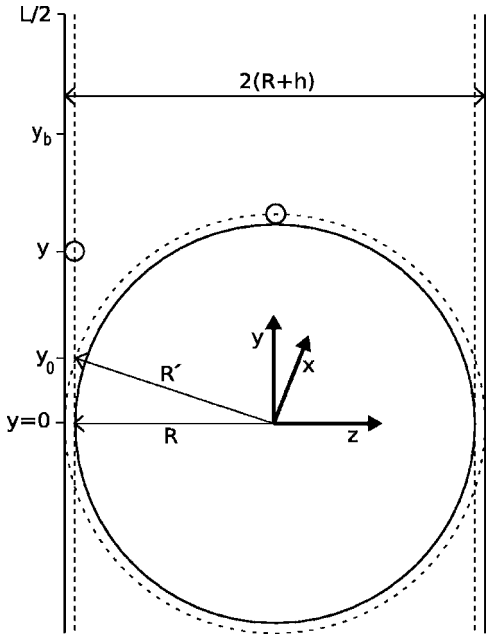

FIG. 1. A scale drawing of a slice at $x=0$ (the yz plane) through the annular geometry adopted for our simulation systems. To save space the bottom section of the figure is truncated. Solid lines represent the physical hard-wall boundaries of the planar walls and the fixed central colloid. The dashed lines are the associated exclusion boundaries for hard-sphere solvent; i.e., the limits of closest approach for the center of a solvent sphere of diameter σ (as illustrated). Periodic boundaries were placed at $x=\pm L/2$ and $y=\pm L/2$; not drawn. The simulation box therefore has dimensions $L \times L \times 2(R+h)$ and aside from the far corners is dominated by annular symmetry about the z axis.

structure of the adsorbed solvent is no longer influenced by the annular geometry; i.e., at $y > y_b$ the density profile $\rho_w(y;h) \equiv \rho(y, z \to z_w; h)$ of solvent adsorbed on the hard walls $[z_w = \pm(R' + h - \sigma)]$ is the constant ρ_w belonging to a planar wall-solvent interface. The above notation also reminds readers when the density profile is implicitly dependent on the distance h between the colloid and the wall. For all our simulations reported below we were able to maintain the fixed value $y_b = 14.5\sigma$. Periodic boundary conditions were imposed at $x = \pm L/2$ and $y = \pm L/2$, with $L/2 = 20.5\sigma$ chosen to be significantly greater than y_b. We can therefore regard the two annular wedges to be independent and to be bounded by reservoirs of semi-infinite wall-solvent regions including a significant amount of homogeneous bulk solvent; note that from previously published planar wall-solvent simulations we could be confident in advance that overlap of density profile structure from different interfacial regions would be minimal for separations greater than 8σ [15]. We restricted our data sampling to annular symmetry by simply ignoring the unwanted corners of our simulation box. Finally, for our chosen size ratio $2R/\sigma = 20$, note that the separation between the dashed planar boundaries varies between 19σ and 21σ for systems spanning the depletion regime.

Colloid-wall geometry has the considerable advantage over colloid-colloid geometry in that the depletion force measurement (see below) can be restricted to measuring the adsorption of solvent on the planar walls alone. It is unlikely that our conclusions below are restricted to this geometry, since both Derjaguin theory and FMT-DFT predict that for our chosen radius of curvature $R' = 10.5\sigma$ the colloid-wall depletion force is very close to twice the corresponding colloid-colloid result, throughout the entire depletion regime [8]. If, as we shall argue, the Derjaguin approximation is asymptotically exact in the limit of $R' \to \infty$ then so also is the geometric scaling of two, between colloid-wall and colloid-colloid geometry; see, e.g., [10]. The size ratio of 20 is a convenient choice for our simulation method because it allows a nice balance between the various inhomogeneous regions that we require to be in equilibrium with one another, but otherwise independent, and between these regions and homogeneous bulk solvent. This size ratio is also a good choice for studying the disagreement between FMT-DFT and the Derjaguin approximation, since if the analysis of Oettel [11] is valid then it will lie intermediate between the two contrasting predictions. Roth and co-workers have used FMT-DFT to obtain the depletion force in both colloid-wall and colloid-colloid geometry at size ratios between 10 and 50. These data were obtained at a solvent chemical potential corresponding to a reduced bulk density of $\eta \equiv \pi\rho\sigma^3/6 = 0.3$. Since the physics we wish to study is predicted to be extremely evident at higher pressures than this, we have also carried out simulations at $\eta = 0.4$ for comparison with the FMT-DFT data of Goulding [9]. Oettel has confirmed that the results of these two earlier studies are not significantly dependent on various modifications of FMT-DFT, including additional statistical mechanical consistency [11]. There are two important predictions shared by all these density functional studies of the depletion force of hard-body models. First, the depletion force $f(h)$ is not a linear function of h and, in particular, at moderate to high pressure the nonlinearity is extreme in the repulsive region $h \to \sigma$. Second, this nonlinearity is not a function of colloid radius; i.e., the scaled depletion force $f(h)/R'$ is found to be essentially independent of size ratio (at least in the range studied to date; $10 \leqslant 2R/\sigma \leqslant 100$).

Our simulations were performed with standard Monte Carlo procedures in the grand canonical ensemble [16,17]. This choice was made so that we could set the chemical potential μ of the solvent to desired values. Note that canonical ensemble simulations would be inappropriate for our complex annular geometry, since adsorption in each wedge and along the planar and colloid surfaces would cause unacceptable difficulties in setting the required thermodynamic state (bulk density of solvent). Solvent insertions and deletions were made with equal probability throughout the simulation box, which means that in effect we relied on mechanical equilibrium with the rest of the system to ensure equilibrium deep within the narrow confines of the wedges. That is each annular wedge subsystem of our total simulation system is in contact with a large reservoir at a fixed chemical potential. In Sec. III below we describe measurements of the average quasi-two-dimensional density confined deep within the center of the wedges, together with density profiles along the planar walls and associated fluctuation phenomena, which attest (or otherwise) to the success of this approach. We used a two-stage approach to equilibrating systems of the geometry of Fig. 1. The first stage involved equilibrating a system of hard-sphere fluid bounded by the planar hard walls and periodic boundaries depicted in Fig. 1, but with no colloid present. The fixed colloid was then introduced into an equilibrated planar geometry configuration, by simply deleting all solvent spheres overlapping with the central colloid (solvent coordinates that lay within a radius of R' of the colloid center). A second period of equilibration was then carried out in annular geometry to allow for adsorption and desorption into and out of the wedge regions. Depending on the choice of chemical potential (and hence bulk pressure p) and the value of h these two stages required up to 2×10^8 and 4×10^9 simulation steps, respectively; each step defined as one translation attempt of a randomly chosen solvent. In addition, one attempt to either insert or delete a solvent sphere (placed or chosen at random throughout the system) was made after every tenth step. Typical production runs at a fixed colloid-wall separation were split into ten subaverages (for statistical error estimation purposes) each subaverage of length 10^8 at $\eta = 0.3$ and length 2×10^8 at $\eta = 0.4$. These systems were sampled 1000 times per subaverage to collect density profile data (see below). In addition, for each choice of chemical potential a giant simulation run was carried out at $h = \sigma$ only. The production runs of giant simulations consisted of 50 subaverages at $\eta = 0.3$ and 100 at $\eta = 0.4$, each subaverage of length 4×10^8. The total amount of solvent in our production systems depended on the set values of h and μ, but was always within the range $16\,000 < N < 25\,000$.

Our simulation method relies on the following statistical mechanical sum rule expressing mechanical equilibrium of solvent adsorbed in a single annular wedge, in the form of a wall-fluid virial theorem [5,10,18]:

$$\beta f(h) = \beta p \frac{\partial V(h)}{\partial h} + 2\pi \int_{y_0}^{\infty} dy y [\rho_w(y;h) - \rho_w], \tag{2}$$

where β denotes the inverse temperature $1/T$ in units of Boltzmann's constant k_B. In the absence of the colloid this result reduces to the planar hard-wall sum rule [19]

$$\beta p = \rho_w. \tag{3}$$

The first term on the right side of Eq. (2) is the direct contribution of the depleted volume that is denied to solvent centers within the wedge, and can be calculated directly from Fig. 1:

$$\frac{\partial V(h)}{\partial h} = -2\pi R'(\sigma - h) + \pi(\sigma - h)^2. \tag{4}$$

Note that this result is the single wedge value, exactly one-half that for the double wedge geometry of Fig. 1. The remaining integral term on the right of Eq. (2) is the total excess number of particles in contact with one of the planar walls (a two-dimensional adsorption), which hereafter will be denoted I_w. In simulation code I_w is expressed in the form

$$I_w = \frac{1}{\delta} \langle N_w \rangle_{\lim \delta \to 0} - \rho_w A_w, \tag{5}$$

where N_w counts the number of solvent centers lying in a bin of depth δ directly adjacent to one of the planar walls (the planar dashed boundaries in Fig. 1) and the angular brackets denote a grand canonical statistical average. $A_w = \pi[(L/2)^2 - y_0^2]$ refers to the area of the wall forming the sides of this giant annular bin. So, measurement of the depletion force simply requires us to collect the average amount of solvent present within a series of such bins of different depth and then extrapolate to zero bin depth. The same extrapolation restricted to the region $y_b < y < L/2$ enabled us to directly measure ρ_w and hence the bulk pressure. In practice, this extrapolation was always readily carried out with only four data points required ($\delta/\sigma = 0.02$, 0.04, 0.06, and 0.08) and essentially introduced no additional numerical error because of the simple one-body nature of the integrand. The statistical error reported below is therefore dominated by natural density fluctuations within the system as a whole. The only other aspect of the measurement is that we must also subtract off the value that would be found in the absence of the colloid; $\rho_w A_w$. This can be done in two ways, either directly measure the same quantity restricted to the range $y_b < y < L/2$, or from Eq. (3) insert the pressure defined by the bulk equation of state at our chosen thermodynamic state.

In the Derjaguin approximation it is straightforward (see, e.g., [10]) to show that I_w evaluates to $-4\pi R' \beta\gamma$, where γ denotes the surface tension of an isolated wall-solvent interface (within the spirit of the Derjaguin approximation one should ignore the insignificant curvature dependence of the colloid-solvent surface tension). For our hard-body model we have access to quasiexact analytic expressions for the thermodynamic quantities that fully determine the depletion force in the Derjaguin approximation [20]:

$$\pi \beta p \sigma^3 = \frac{6\eta(1 + \eta + \eta^2 - \eta^3)}{(1 - \eta)^3}, \tag{6}$$

and [21]

$$-4\pi\beta\gamma\sigma^2 = \frac{18\eta^2\left(1 + \frac{44}{35}\eta - \frac{4}{5}\eta^2\right)}{(1 - \eta)^3}. \tag{7}$$

We stress that measurement of I_w and hence the depletion force does not require us to collect data within a grid of annular bins, since it is only the total amount of solvent at the wall that is required to evaluate the sum rule. Nevertheless, we also collected a graphical representation of the solvent density profile along the wall $\rho_w(y;h)$, for each fixed value of colloid-wall separation h, by recording data within a large number of annular simulation bins lying adjacent to the planar walls, all of fixed depth $\delta = 0.02\sigma$ and radial extension $\delta y = 0.1\sigma$. For this purpose it was neither necessary nor sensible to develop an extrapolation procedure at each value of y and therefore this measurement did not probe deep within the wedge ($y \to y_0$). Instead, to measure the quasi-two-dimensional density near the central portion of a wedge we averaged the entire amount of solvent within the wedge $\langle N \rangle(y)$, from y_0 out to a distance y, to define the quantity

$$\rho_{2d}(y) \equiv \frac{\langle N \rangle(y)}{\pi(y^2 - y_0^2)}. \tag{8}$$

Another sum rule for the depletion force, or rather its isothermal derivative with respect to chemical potential, can be obtained from the Gibbs adsorption equation for the entire simulation system:

$$\frac{\partial f(h)}{\partial \mu} = \rho \frac{\partial V(h)}{\partial h} - \frac{\partial \gamma}{\partial \mu} \frac{\partial A(h)}{\partial h} + \frac{\partial \langle N^{ex} \rangle(h)}{\partial h}. \tag{9}$$

As with sum rule (2) we have expressed this exact result fully in terms of quantities appropriate to a single annular wedge (one-half of the simulation system depicted in Fig. 1). Thus $\langle N \rangle^{ex}$ is the excess adsorption within a single annular wedge, left after the bulk density ρ and planar surface adsorptions $-\partial\gamma/\partial\mu$ have been subtracted. This is a line adsorption defined from the line tension (free energy) of the annular wedge [22]. We report data from this adsorption route in Sec. IV, in addition to our measurements of the depletion force via sum rule (2).

III. STRUCTURE OF HARD-SPHERE FLUID ADSORBED IN A HARD-ANNULAR WEDGE

This section presents highlights and representative samples from the structural data measured in our simulation runs to describe key features of the density distribution of hard-sphere fluid adsorbed in a hard-annular wedge. Because of the nature of the virial theorem (2) the density profile along the walls is directly associated with mechanical equilibrium in annular geometry. Figure 2(a) shows a representation of this profile, from the giant simulation run at $h = \sigma$ for the high pressure state $\eta = 0.4$. Although we have not at-

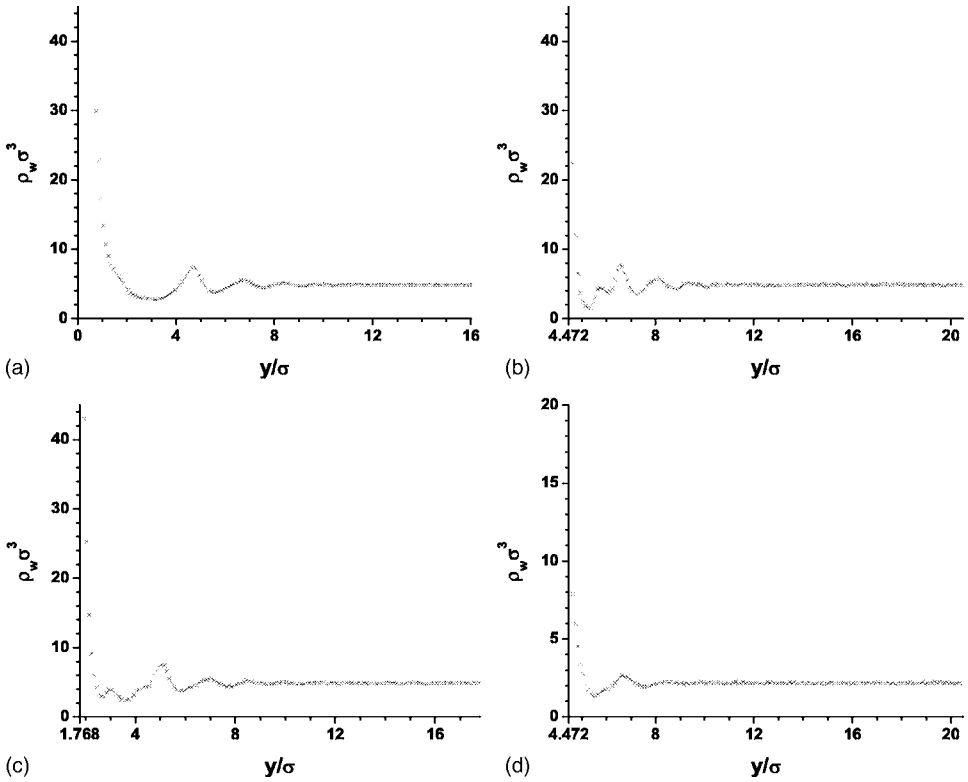

FIG. 2. Density profiles along the planar walls of our annular wedge systems. The data are averaged over annular bins in contact with the planar boundaries, of radial extent 0.1σ and depth 0.02σ. We have not attempted to collect data for values of y too close to y_0 because this procedure would require bins of smaller depth. (a) At $h=\sigma$ for the thermodynamic state $\eta=0.4$. (b) At $h=0$ for the thermodynamic state $\eta=0.4$. (c) At $h=0.85\sigma$ for the thermodynamic state $\eta=0.4$. (d) At $h=0$ for the thermodynamic state $\eta=0.3$.

tempted to extrapolate this data to the limit of the wall boundary (it is raw data collected in annular bins of thickness 0.02σ out from the planar walls) Fig. 2(a) is nevertheless a strong indicator of the structure of $\rho_w(y;h=\sigma)$. The dramatic rise in the center of the wedge is simply a consequence of the quasi-two-dimensional geometry in this region. For a planar pore of width $h=\sigma$ the density can be calculated analytically from Widom's potential distribution theorem [23], which implies that in an open system the three-dimensional density ρ remains finite even though the volume available to solvent centers has shrunk to zero; $\rho\sigma^3=\exp(\beta\mu)$ [19]. This, in turn, implies that the two-dimensional density ρ_{2d} is zero; i.e., the structure has reduced to a two-dimensional ideal gas. From the equation of state (6) at $\eta=0.4$, $\exp(\beta\mu)$ evaluates to the very high but nevertheless finite value of 6424, which is an upper bound for $\rho_w(y=0;h=\sigma)\sigma^3$ in our annular wedge system. Obviously, the numerical procedure used to generate Fig. 2(a) is not able to probe this limit; instead, we shall report values of ρ_{2d} defined by Eq. (8) to explore the quasi-two-dimensional region $y<\sigma/2$.

Another outstanding feature of the density profile of Fig. 2(a) is the separation of successive peaks. Typically, density profiles show dominant structural correlations on the length scale of the solvent diameter σ. Here, the first peak beyond the center of the wedge, which we shall denote as $y=y_1$, does not appear until $y_1=4.7\sigma$. We can understand this result in terms of structure induced across the annular wedge, as opposed to structure along the walls, as depicted in Fig. 3. This figure depicts the range of solvent-solvent separations associated with a pair of solvent spheres becoming temporarily jammed across the annular wedge; i.e., one sphere is sitting on the planar wall at annular radius y_1 while another sphere is directly across the wedge on the colloid surface. In particular, the separations S_1 and S_2 defined in Fig. 3 are solutions of

$$R'^2 = y_1^2 + (R' + h - \sigma - S_1)^2, \tag{10}$$

$$(R' + S_2)^2 = y_1^2 + (R' + h - \sigma)^2. \tag{11}$$

Inserting $y_1=4.7\sigma$ and $h=\sigma$ into these equations yields $S_1=1.111$ and $S_2=1.004$. These values confirm that the peak at $y=y_1$ arises from correlations due to confinement across the annular wedge. Successive peaks are also separated by non-integer values of σ, up until $y=8\sigma$ where solvent is no longer significantly confined within the wedge, as one would also predict from the Derjaguin approximation [10]. An identical correspondence was found at all values of h within the depletion regime. For example, at the opposite extreme $h=0$ the dominant peak lies at $y_1=6.6\sigma$ [see Fig. 2(b)] corresponding

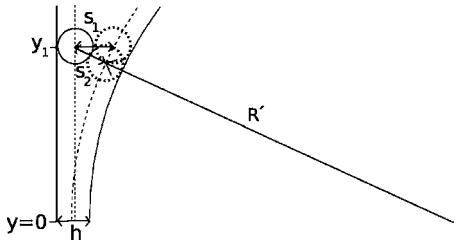

FIG. 3. An illustration of configurations in which a pair of solvent spheres of diameter σ are temporarily jammed across an annular wedge. One sphere lies on the planar wall at $y=y_1$ while the dotted spheres show a range of positions for a sphere on the colloid wall. Double headed arrows labeled S_1 and S_2 denote separations of jammed pairs.

to $S_1=1.33$ and $S_2=1.07$. At $h=\sigma$ one can notice two shoulders lying deep within the annular wedge, which can only be due to correlations in the plane of the wall. For all $h \leqslant 0.95\sigma$ one or both of these shoulders becomes a small but recognizable peak at radial distances from y_0 that hardly vary at all with h; see Figs. 2(b) and 2(c). Thus in the nanocolloidal regime at least, there must exist some contribution to the depletion force from correlations induced along the walls. At the lower pressure state $\eta=0.3$ the same scenario is observed, but the structure is noticeably weaker; Fig. 2(d).

For the giant run of Fig. 2(a) there is no sign of statistical error in the wall density profile, on the scale of the figure. One does observe minor statistical error in the remaining plots, from our standard runs, but is perhaps less than one might have expected. However, when we compared the wall density profiles from subaverage to subaverage and between left and right annular wedges, from our standard runs, there was a striking appearance of statistical error at all radial distances, as if the density profile was shifting up and down the wedge by around 0.2σ over the length of roughly one subaverage. If this is not an illusion, then Fig. 3 is presumably the explanation; i.e., in an annular wedge the structure is constantly adjusting between unfavorable and favorable correlations across the wedge. This is probably also the reason why the amplitude of the oscillatory structure along the walls decays so quickly, even at relatively high bulk pressure; note, for example, that the data of Fig. 2 are fully supportive of our choice of $y_b=14.5\sigma$ as shown in Fig. 1. From the depletion force data (measured values of I_w), described in Sec. IV below, it was clear that structural rearrangements within the annular wedges could sometimes be quite violent, presumably due to the sudden formation of collective annular density waves. Such major events, if they occurred, took around three standard-run subaverages to settle down and so the depletion force data from standard runs is subject to significant statistical error. Note, however, that this error is due entirely to natural fluctuations on the typical time scale of a subaverage and so is properly averaged over by considering many runs or undertaking single giant runs. Evidence for the collective nature of these fluctuations is seen in Sec. IV by comparing the data for the depletion force between the two routes to determine ρ_w, defined above. If the wavelength of the density/pressure fluctuations along the wall are of the order of y_b then the wedge and bulk regions will typically suffer opposite deviations, which will make the average of the two routes lie closer to the fully equilibrated value than either of the routes separately.

One concern regarding simulations of solvent adsorbed in highly confining wedges is that the confinement might conceivably induce crystallization at the walls, within the wedge [24]. To rule this possibility irrelevant to our data, we collected occasional snapshots of the positions of solvent spheres lying within 0.02σ of the solvent walls; one for each planar wall, per subaverage. A few representative examples from the high pressure system are shown in Fig. 4. In particular, we never observed long-term structure of any class within this first adsorbed layer. Instead, the number and distribution of solvent spheres lying deep within the annular wedge appears to vary extensively from snapshot to snapshot and between the two wedges. At $h=\sigma$ some snapshots were

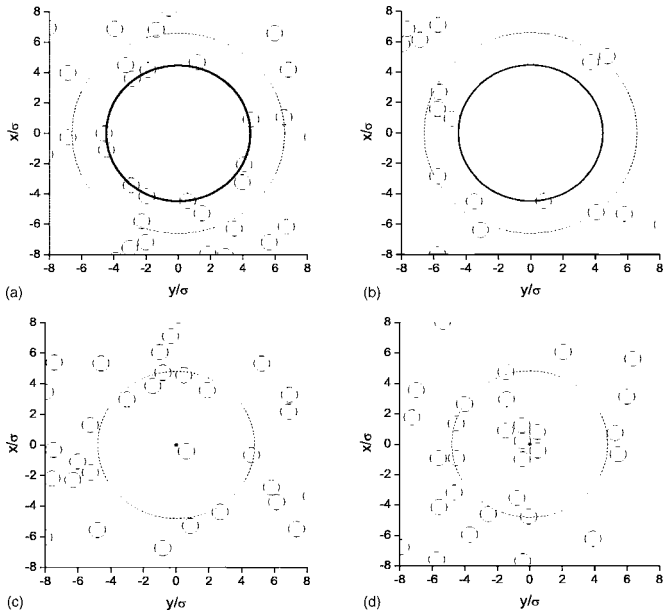

FIG. 4. Snapshots of solvent spheres projected onto the planar walls of our annular wedges. Only solvents whose centers lie within a depth 0.02σ from the wall are plotted (as circles of diameter σ). Thick black circles (shrinking to a point for $h=\sigma$ systems) denote the apex of the wedge (the inner boundary $y=y_0$ for solvent centers). Dashed circles represent the outer boundary of the quasi-two-dimensional region at the center of the wedges (at radius y_1 in Fig. 3 as obtained from the main peaks in Fig. 2). (a) At $h=0$ from the high pressure system $\eta=0.4$. (b) A configuration contrasting with that shown in (a) from the same system. (c) At $h=\sigma$ from the high pressure system $\eta=0.4$. (d) A configuration contrasting with that shown in (c) from the same system. Both pairs of configurations are separated by at least one subaverage.

consistent with a quasi-two-dimensional ideal gas inside the wedge [Fig. 4(c)] but just as many other snapshots showed significant adsorption [Fig. 4(d)]. At $h=0$ one sees similar dramatic variations in the amount of adsorbed solvent present close to the apex of the wedge [the thick dark circles in Figs. 4(a) and 4(b)]. The dotted circles are drawn at $y=y_1$ as defined in Fig. 3, which can be regarded as the outer "wall" of the quasi-two-dimensional region. Of course, these snapshots are restricted to a small region near the planar walls and could therefore be misleading as to the amount of solvent in the wedge; as it clearly is outside the wedge. For this purpose, we measured the quasi-two-dimensional density defined by Eq. (8). Figure 5(a) shows this data for the $h=\sigma$ wedges at $\eta=0.3$ and 0.4, from giant runs of 50 subaverages each. One observes that the density does indeed become gaslike in the central region of the wedge, but nevertheless at our chosen radius of curvature R' there is sufficient density to allow for collisions between spheres on opposite sides of the center of the wedge (which at $h=\sigma$ is really an annular slit pore rather than a wedge).

This physics, dominant for $h \to \sigma$, has been proposed as a possible reason for the breakdown of the Derjaguin approximation for the depletion force, in the repulsive force region only [10]. It plays a central role in the modeling of Oettel [11] which extends the Derjaguin approximation by explic-

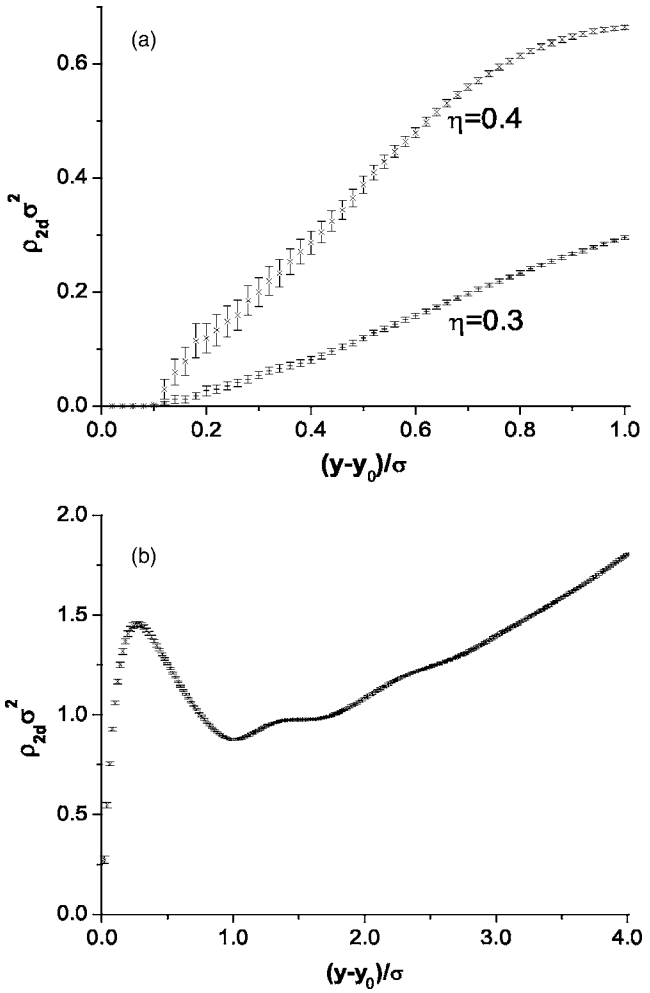

FIG. 5. Average number of solvent spheres adsorbed out to a radius y from the wedge apex y_0, divided by the area of this region projected onto the xy plane, defining an average effective two-dimensional density, Eq. (8). (a) At $h=\sigma$ ($y_0=0$) for the thermodynamic states $\eta=0.3$ and $\eta=0.4$. (b) At $h=0$ for the thermodynamic state $\eta=0.4$.

itly treating the quasi-two-dimensional region of the wedge with two-dimensional scaled particle theory. Our data in Fig. 5(a) appear to be consistent with this modeling and we shall return to this issue in Sec. IV. As with all our measurements of solvent content deep inside the wedge, these data showed great variation between successive subaverages, implying large fluctuations in content on the time scale of a typical subaverage. For example, at $h=\sigma$ ($y_0=0$) even for the high pressure system, there was sometimes no solvent present within a radius of $y=0.3\sigma$ from the center of the wedge/pore over an entire subaverage, while at other times the subaverage value up to $y=0.2$ was more than twice its fully equilibrated value. Despite these fluctuations, our simulation procedures could not equilibrate a density structure at $y\leqslant 0.1\sigma$ inside the $h=\sigma$ wedge/pore, even during a giant run, because the probability of a solvent center entering this region was too small to be sampled by our standard Monte Carlo algorithm. From the potential distribution theorem applied to very thin pores [19] one would expect smooth behavior for $\rho_{2d}(y\rightarrow 0)$ but the probability of a sphere penetrating this far was so small that it did not happen even once during our giant runs. It seems clear from Fig. 5(a) that this cannot effect our depletion force measurements at $\eta=0.3$ and from Oettel's modelling is at worst marginal at $\eta=0.4$ [25]. We conjecture that in a bulk colloidal system, where the colloids are moving, it is plausible that this apparent lack of ergodicity is accentuated. We also conjecture that this behavior is linked to the structure seen in Fig. 5(b), which plots $\rho_{2d}(y)$ from our $\eta=0.4$ system at $h=0$. This figure shows what appears to be a kinetic barrier (the large peak) as if solvent arriving deep within the wedge sees an effective annular wall due to other solvent that has failed to penetrate the extremely narrow confines. One also observes outer bumps at a spacing of roughly σ, which confirm the presence of structure induced parallel to the walls, as previously surmised from Fig. 2(b). Otherwise, the quasi-two-dimensional density at $h=0$ falls dramatically close to the apex, as expected from the potential distribution theorem, although the larger opening angle of this wedge allows solvent to penetrate much further.

IV. RESULTS FOR THE DEPLETION FORCE OF HARD-BODY COLLOIDAL PHYSICS

Figure 6 displays our simulation results for the depletion force, in comparison with FMT-DFT, the Derjaguin approximation, and a modification of the latter based on Oettel's modeling [11]. For completeness Fig. 6(b) replots our previously published data [6,26] at $\eta=0.4$, together with a more detailed illustration of our interpretation based on the analysis of Oettel. Open circles are obtained from direct measurement of the integral on the right of sum rule (2) while the associated crosses use the same value for the first half of the integral but adopt the limiting value of ρ_w defined by the bulk equation of state (3) and (6). The density fluctuations described in Sec. III are responsible for the significant error bars (from standard runs). The fact that the average between the two routes (circles and crosses) is a smoother indication of the true result is illustrated in Fig. 6(b) at $h=0.9\sigma$ by plotting two pairs of points. The lowest circle and the highest cross are the data from all ten subaverages. The large disparity for this system was readily traced to a major fluctuation that occurred during the seventh subaverage, that did not recover until the end of the simulation. The much closer pair of points in the middle are the result of restricting the averaging to the first six subaverages, which did not suffer a major out of equilibrium event. Overall our standard simulation runs occupy the space in between the Derjaguin prediction (straight line) and the results of FMT-DFT (full curves). As we believe that our simulations are correctly sampling physical time scales if averaged over sufficient numbers of standard subaverages [27] it already follows that neither FMT-DFT nor the Derjaguin approximation are valid in the repulsive force regime at this size ratio. To be absolutely certain of new physics present at $h=\sigma$ we undertook giant runs for this separation alone. These giant runs were more than an order of magnitude longer than all our other data combined and have an associated statistical error less than the size of the plotted symbol (small closed diamonds labeled with our chosen colloid/solvent size ratio of 20).

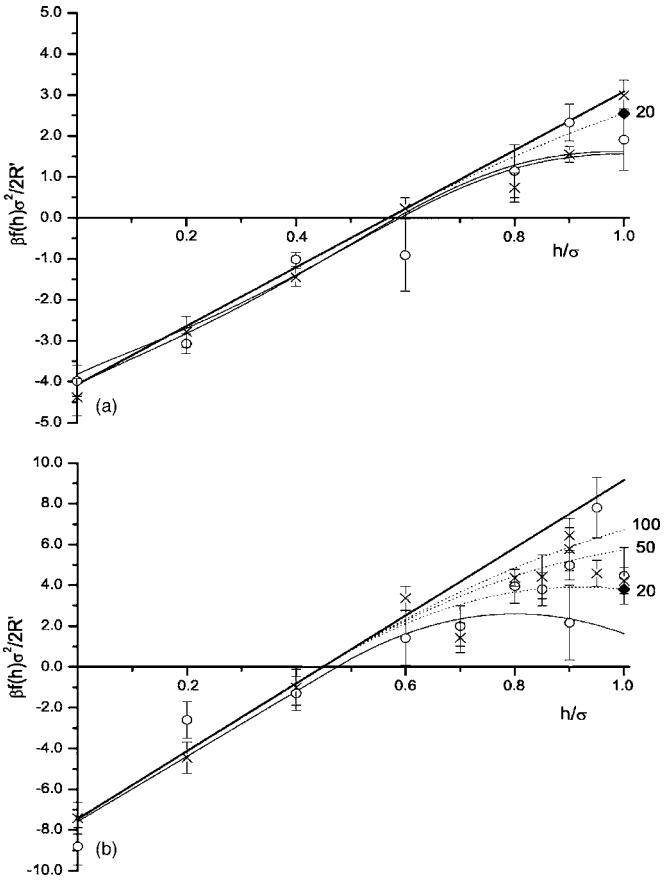

FIG. 6. Depletion force of colloidal hard-sphere models, scaled with the effective colloid diameter. Symbols with error bars display our simulation data; see text. Straight lines depict the Derjaguin limit of mesoscopic colloidal size. Full curves show FMT-DFT data. The dotted curves are based on the analysis of Oettel [11]. Those labeled 20 can be regarded as physically based representations of our simulation data in the absence of statistical error; see text. (a) At $\eta=0.3$, with FMT-DFT data from Ref. [8]. The latter consist of two closely spaced curves for size ratios 10 and 50, respectively. (b) At $\eta=0.4$, with FMT-DFT data from Ref. [9].

In Fig. 6(a) the thermodynamic state is $\eta=0.3$ corresponding to a moderate bulk pressure and has been extensively studied before by colloidal mixture simulations and integral equation theories [12–14], as well as FMT-DFT. For the comparison with FMT-DFT in Fig. 6(a) we have chosen the data of Roth *et al.* [8,28]. These authors directly confirmed that when scaled linearly with colloid radius (as plotted) their FMT-DFT data was almost indistinguishable at size ratios as disparate as 10 and 50. They also demonstrated that FMT-DFT shows an almost perfect geometric scaling between colloid-colloid geometry and colloid-wall geometry (the same factor of 2 predicted by the Derjaguin approximation). Oettel has also confirmed these scaling properties of FMT-DFT for size ratios up to 100 [11]. There is therefore no sign that the qualitative disagreement with the Derjaguin approximation in the repulsive force region might reduce at increasing size asymmetry. The same comparison at $\eta=0.4$ [Fig. 6(b)] shows that this disagreement becomes dramatic at higher pressure. Here, the only FMT-DFT data we have available for comparison is that from Goulding's thesis [9]; but see also Ref. [11]. Exactly the same features are seen at both thermodynamic states but, due to the relative insensitivity with pressure of the statistical error in our simulation data, Fig. 6(b) presents the most convincing evidence of the existence of new physics not captured by either the Derjaguin approximation nor FMT-DFT [6]. Additional values of h were therefore sampled at $\eta=0.4$. Nevertheless, the giant run at $\eta=0.3$ does highlight the qualitative disagreement between our simulations and FMT-DFT, showing that the problem is present even at moderate pressure.

If we accept Oettel's proposal [11], at least qualitatively, then the difference between our data and the Derjaguin limit, on the one hand, and FMT-DFT data on the other, is due to a line tension contribution that is missed altogether by the Derjaguin approximation while grossly overestimated by FMT-DFT. This further implies that we should be able to link our data to these two limiting forms by the introduction of a single additional parameter (representing the disparity with the Derjaguin approximation at $h=\sigma$). To achieve this requires us to first fit our data with a function identical in form to the FMT-DFT prediction. In fact, the FMT-DFT data of Ref. [9] are remarkably well-fitted by a straight line at negative depletion force and a quadratic curve for the repulsive region, spliced together with matching slopes. The same procedure leads uniquely to the dashed curves in Fig. 6, having fixed the value at $h=\sigma$. It should be noted that this unification cannot be exact because it ignores some minor curvature in the attractive force region [8] (apparently also ignored in [9]) that is not the subject of our study, and the fact that the Derjaguin limit already contains some minor cancellation of errors at nanocolloidal size ratios. Notwithstanding, in Fig. 6(b) the only discernible difference between our representation of the FMT-DFT data of [9] and the original data is that the latter shows a hint of a dimple in the close vicinity of $h=\sigma$. The values of I_w obtained from the giant runs at $h=\sigma$ fully determine the fits to our simulation data. These fits are clearly in good agreement with the results of our standard runs, despite the large error bars associated with individual data points. We can now use our fitting procedure to illustrate the nature of the fan predicted by Oettel; i.e., the nature of the convergence to the two limits as the size ratio is varied:

$$\frac{\beta f\sigma^2}{2R'} = \frac{I_w^\infty \sigma^2}{2R'}\left(\frac{h-h_0}{\sigma-h_0}\right)\left[1-\frac{I_w^\infty - I_w(\sigma)}{I_w^\infty}\left(\frac{h-h_0}{\sigma-h_0}\right)\right];$$

$$h_0 \leqslant h \leqslant \sigma, \tag{12}$$

where $I_w(\sigma)$ refers to the value at $h=\sigma$, $I_w^\infty\sigma^2/2R' = -2\pi\beta\gamma\sigma^2$ denotes the Derjaguin limit of large R' and

$$\frac{\sigma-h_0}{\sigma} = \frac{I_w^\infty\sigma^2/2R'}{\pi\beta p\sigma^3}. \tag{13}$$

We might expect from Eq. (1) that for sufficiently large size asymmetry

$$\frac{I_w^\infty - I_w(\sigma)}{I_w^\infty} = \alpha(\eta)\sqrt{\frac{\sigma}{2R'}}. \tag{14}$$

Setting the value of the coefficient from our giant run at high pressure yields $\alpha(0.4)=2.68$ from a size ratio of 20. Figure

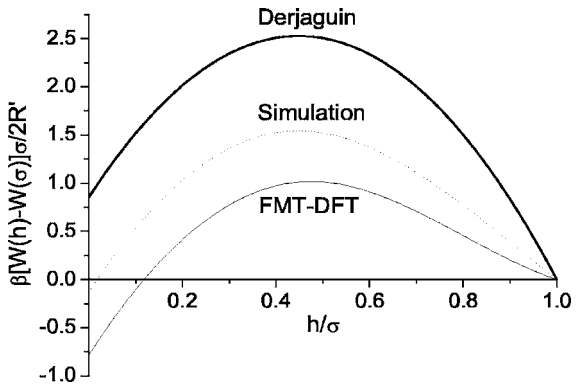

FIG. 7. Depletion potentials, obtained from the area under the depletion force curves displayed in Fig. 6(b).

6(b) also displays curves at size ratios of 50 and 100 that illustrate the slow convergence towards the Derjaguin limit resulting from a $\sqrt{\sigma/2R'}$ correction. If we now push this fitting towards molecular sized colloids, then the FMT-DFT data correspond to a size ratio of around 9 or 10. It could therefore be of considerable importance that the depletion force from FMT-DFT has been firmly reported as showing no significant departure from scaling with colloid radius at size ratios from 10 upwards [8,11]. However, the analogous treatment of our data at $\eta=0.3$ shows a more interesting side to this qualitative disagreement. Namely, at this moderate pressure our simulation data are much closer to the Derjaguin limit $[\alpha(0.3)=0.784]$, whereas the FMT-DFT data are a lot further away; corresponding to a size ratio of between one and two. We conclude that the incorrect behavior of FMT-DFT for the repulsive part of the depletion potential is qualitatively present at all but very low pressure, where it reduces to the Derjaguin limit. So, at moderate pressure the Derjaguin approximation is significantly better than FMT-DFT, in relative terms, while at high pressure the nanocolloidal regime is pushed relatively closer to the FMT-DFT prediction, although the absolute error is increasing with pressure. Why then have previous authors reported good agreement with the same FMT-DFT data at $\eta=0.3$? The answer can be seen in Fig. 6(a), where one notes that within simulation error it is tempting to put a straight line through the data such that the difference with the FMT-DFT curve is minimized, although this will then have a significantly smaller slope than the Derjaguin value [10]. When translated into the depletion potential, the area under the depletion force curves of Fig. 6, the qualitative disagreement with the FMT-DFT prediction is no longer obvious, due to the cancellation of error involved in replacing the incorrect curvature of the FMT-DFT prediction with a straight line of unphysical slope. We return to some of these issues concerning fitting of the simulation data in the discussion section below.

Figure 7 displays the depletion potentials $W(h)$ defined by the depletion forces plotted in Fig. 6(b). At this high pressure the Derjaguin approximation predicts no stable depletion attraction, instead a minimum lies at $h=\sigma$. In contrast, FMT-DFT continues to show a strong depletion attraction at contact with the wall. Our simulation system at a size ratio of 20 lies almost exactly on the boundary between these two qualitatively different regimes. The zero of the depletion potential is not determined from force measurements, but from comparisons of FMT-DFT with the Derjaguin approximation [9] we expect that the value at the origin $W(0)$ varies much more than $W(\sigma)$. Accordingly, we have chosen to plot $W(h)-W(\sigma)$.

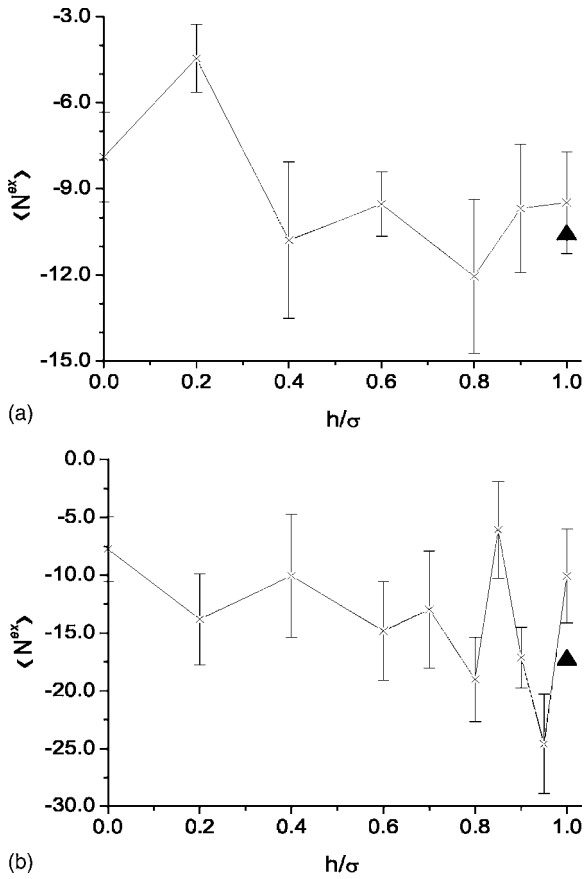

FIG. 8. Excess line adsorption of solvent within an annular wedge, defined by the decomposition (15). Straight lines joining successive data points are just guides to the eye. The solid triangles denote giant run values at $h=\sigma$; here the symbol size is the error bar. (a) At $\eta=0.3$. (b) At $\eta=0.4$.

Another route to the depletion force is via the Gibbs adsorption equation (9). In the grand canonical ensemble [29] this simply requires us to measure the average total number of solvent particles in the system:

$$\langle N\rangle \equiv \rho V(h) - \frac{\partial \gamma}{\partial \mu} A(h) + \langle N^{ex}\rangle(h). \tag{15}$$

In particular, defining $\Delta f \equiv f - f^{\infty}$ where f^{∞} denotes the Derjaguin limit of mesoscopic colloid radius,

$$\frac{\partial \Delta f}{\partial \mu} = \frac{\partial}{\partial h}\langle N^{ex}\rangle. \tag{16}$$

Figure 8 shows our data for the excess line adsorption $\langle N^{ex}\rangle(h)$ in a single annular wedge. It is notable that this line adsorption is very small; a deficit of only about ten solvent particles per annular wedge. Since this is of order 0.1% of the total amount of solvent, the data from standard runs are

not accurate enough to make this route practical. In fact, within the statistical error of our standard runs it is not possible to discern any dependence on h, even at $\eta=0.4$, and hence confirm a deviation from the Derjaguin limit. We can argue that this null result is not in contradiction with our direct measurements of the depletion force, within statistical error, by considering our giant run results at $h=\sigma$. A rough estimate of the left side of Eq. (16) is $[\Delta f(\eta=0.4)-\Delta f(\eta=0.3)]/[\mu(\eta=0.4)-\mu(\eta=0.3)]\simeq -23/\sigma$ which is not inconsistent with the data in Fig. 8. Also, this route clearly suffers from the possibility that $\partial\Delta f/\partial\mu$ might well be a strong function of h.

V. DISCUSSION

Our simulation data are restricted to a size ratio of 20. With one or two orders of magnitude more simulation time, it would be possible to be fully predictive as to the precise form of the depletion force in hard-body colloidal physics. In particular, giant simulation runs carried out over the full range of separations h would allow one to probe the limitations of the simple quadratic extension to the Derjaguin form, and giant runs at separation $h=\sigma$ for a range of size asymmetry are needed to confirm the $\sqrt{R'}$ scaling prediction of Oettel's modeling. Notwithstanding, it is already clear from our current data that neither the Derjaguin approximation nor FMT-DFT as previously implemented are able to correctly describe the depletion force of hard-body colloidal systems in the nanocolloidal regime. Since the Derjaguin approximation is one of the foundation stones of colloidal science and FMT-DFT is the most advanced numerical theory of the liquid state currently available, our main conclusion represents a serious challenge to current statistical mechanical understanding of colloidal systems. The pair depletion force is the dominant short-range interaction between colloids even at high concentration of solute and a failure to properly describe this interaction at moderate to high total density makes it impossible to trust predictions of colloidal crystallization in bulk or at surfaces. A similar comment applies to the prediction of interfacial phase diagrams, such as layering and wetting phenomena. The problem might be largely restricted to hard-body models, if due more to the high pressure rather than confinement of solvent. However, the inclusion of attractive interactions would introduce wetting and drying phenomena deep within the annular wedges, between colloids and between colloids and walls, which could easily introduce physics that is not present in either the Derjaguin approximation nor FMT-DFT applied to colloidal mixtures. One must therefore be prepared for colloidal physics to present us with intrinsically harder problems than standard liquid state physics. This warning is likely to be equally relevant to integral equation theories [6,12,13,30].

Oettel's proposed extension to the Derjaguin approximation [11] appears to show considerable promise. By explicitly modeling the quasi-two-dimensional region deep within the wedge as an annular pore, but still treated in the same spirit as a Derjaguin approximation, Oettel obtains what is essentially a line tension contribution to the Derjaguin approximation. This contribution is important only as $h\to\sigma$ and most likely scales nonanalytically in the curvature; as $\sqrt{\sigma/2R'}$. In this manner, Oettel is able to unify the FMT-DFT prediction with the Derjaguin limit of large size asymmetry. It is obvious why the standard Derjaguin analysis of depletion scales linearly with colloid radius. It is not obvious why this linear scaling is also obtained numerically in FMT-DFT, unless for some fundamental reason the FMT-DFT mixture functional totally fails to capture the annular geometry of colloidal mixtures. In this scenario one might view the FMT-DFT prediction as the molecular limit $2R'\to\sigma$. Then FMT-DFT and the Derjaguin approximation are opposite limits, with the nanocolloidal regime falling in between. This unification is inevitably associated with a breakdown in the linear scaling with curvature. Thus a plot of the depletion force scaled with colloid radius now shows a fan of curves within the repulsive force region, as the size ratio is varied. Our present simulation data are consistent with this prediction, but not conclusive because they are restricted to a single size ratio. In particular, with regard to our modeling in Fig. 6, based on Eqs. (12)–(14), it is not known when/if the $\sqrt{R'}$ scaling breaks down below a size-ratio of 20, nor whether or not the assumed quadratic form for the repulsive depletion force applies above size ratios of 20. Considering the latter issue, we note that it is unclear to the present authors whether or not the precise shape of the depletion force $f(h)$ is quantitatively predicted by the simplified approach of Oettel. To go significantly further with our simulation method would require more than just a substantial investment in resources, it would also demand large changes in simulation system size and/or geometry that would need to be carefully considered to avoid unwanted introduction of finite size effects on confinement structure and density fluctuations.

The reasons for the qualitative breakdown of FMT-DFT are somewhat mysterious. A detailed analysis of the statistical mechanics of FMT-DFT has indicated a possible fundamental limit to its validity for systems of large size asymmetry [31]. Indeed, these authors specifically warn against trusting FMT-DFT in the depletion regime of colloidal physics, warning of possible inherent "dramatic bias in the case of mixtures of very dissimilar spheres." However, a full understanding of the fundamental basis of FMT-DFT presents formidable challenges in combining geometry with statistical mechanics (statistical geometry) and it is far from obvious how one might go about correcting FMT-DFT without destroying its remarkably useful properties in other applications. Oettel [11] considered a variety of possible improvements, such as imposing the quasiexact bulk equation of state, but reports that these obvious improvements show no convergence to the Derjaguin limit at large size ratio [32]. Of particular interest is the additional statistical mechanical consistency that one can impose on FMT-DFT [11]. The use of FMT-DFT to derive the pair depletion force has been based on the so-called insertion method [8]. This route treats one of the colloids as a fixed external field (a wall) and then calculates the change in solvent grand potential needed to bring a second colloid up to a distance h from the fixed colloid. Here, the underlying statistical mechanics assumes that the FMT-DFT functional for the colloidal mixture is accurate in the limit of zero concentration of colloid in an inhomogeneous solvent. Note that this route only requires solving for

the density profile of pure solvent in the presence of the fixed colloid alone, thereby avoiding the serious numerical problems of minimizing the FMT-DFT functional in annular geometry. Oettel enforces consistency between the insertion route and the low solute concentration limit of a bulk colloidal mixture, but still fails to achieve a qualitative improvement. One might argue from the above that all mixture FMT-DFT functionals are inherently untrustworthy for colloidal systems because they somehow fail to capture the underlying annular geometry. However, this would not apply to FMT-DFT implemented for pure solvent within annular geometry, the direct analog of our simulation procedure, since this "brute force" route only demands accurate modeling of inhomogeneous fluids of pure solvent. The numerical complications of multidimensional DFT are formidable [33], but it would obviously be worthwhile to undertake a direct comparison with our data of Fig. 6(b) despite the fact that it would get us no closer to developing a trustworthy functional for colloidal mixtures.

ACKNOWLEDGMENT

We are very grateful to R. Roth for helpful discussions and for supplying us with the numerical data from Ref. [8] plotted in Fig. 6(a).

[1] *Fundamentals of Inhomogeneous Fluids*, edited by D. Henderson (Marcel Dekker, New York, 1992).
[2] S. Asakura and F. Oosawa, J. Chem. Phys. **22**, 1255 (1954).
[3] A. Vrij, Pure Appl. Chem. **48**, 471 (1976).
[4] Y. Mao, M. E. Cates, and H. N. W. Lekkerkerker, Physica A **222**, 10 (1995).
[5] B. Gotzelmann, R. Evans, and S. Dietrich, Phys. Rev. E **57**, 6785 (1998).
[6] A. R. Herring and J. R. Henderson, Phys. Rev. Lett. **97**, 148302 (2006).
[7] B. V. Derjaguin, Kolloid-Z. **69**, 155 (1934); J. N. Israelachvili, *Intermolecular and Surface Forces* (Academic, London, 1992).
[8] R. Roth, R. Evans, and S. Dietrich, Phys. Rev. E **62**, 5360 (2000).
[9] D. J. Goulding, Ph.D. thesis, University of Cambridge, 2000 (unpublished).
[10] J. R. Henderson, Physica A **313**, 321 (2002).
[11] M. Oettel, Phys. Rev. E **69**, 041404 (2004).
[12] T. Biben, P. Bladon, and D. Frenkel, J. Phys.: Condens. Matter **8**, 10799 (1996).
[13] R. Dickman, P. Attard, and V. Simonian, J. Chem. Phys. **107**, 205 (1997).
[14] E. Allahyarov and H. Lowen, Phys. Rev. E **63**, 041403 (2001).
[15] J. R. Henderson and F. van Swol, Mol. Phys. **51**, 991 (1984).
[16] N. Metropolis, A. W. Rosenbluth, M. N. Rosenbluth, A. H. Teller, and E. Teller, J. Chem. Phys. **21**, 1087 (1953).
[17] M. P. Allen and D. J. Tildesley, *Computer Simulation of Liquids* (Oxford University Press, Oxford, 1987).
[18] P. Attard, J. Chem. Phys. **91**, 3083 (1989).
[19] J. R. Henderson, Mol. Phys. **59**, 89 (1986).
[20] N. F. Carnahan and K. E. Starling, J. Chem. Phys. **51**, 635 (1969).
[21] D. Henderson and M. Plischke, Proc. R. Soc. London, Ser. A **410**, 409 (1987).
[22] D. W. Siderius and D. S. Corti, Phys. Rev. E **71**, 036141 (2005).
[23] B. Widom, J. Chem. Phys. **39**, 2808 (1963).
[24] P. Pieranski, L. Strzelecki, and B. Pansu, Phys. Rev. Lett. **50**, 900 (1983).
[25] In fact, the total adsorption in the annular wedge out to a range of $y=\sigma$ or greater was equilibrated over the time scale of a standard run, so that the sum rule measurement of the depletion force is not affected; see Eq. (5). Instead, Fig. 5(a) implies a slow redistribution of solvent from the region $0.2\sigma<y<0.8\sigma$ into the very central region of the wedge.
[26] Except that the giant run in Ref. [6] is based on a production run at $\eta=0.4$ that is only the first 50 subaverages of the 100 presented here.
[27] At $\eta=0.3$ the average value of ρ_w obtained from all seven simulation systems yielded $\beta p\sigma^3=2.278\pm0.005$ in agreement with the value 2.2768 expected from Eq. (6). At $\eta=0.4$ the same comparison (now over ten systems) is 5.290 ± 0.008 compared with 5.2910. The values of ρ_w obtained from our giant runs were 2.2751 ± 0.0006 and 5.2844 ± 0.0012, respectively. Although the latter differs from Eq. (6) by only 0.13% this is nevertheless more than five standard deviations away. This tiny difference might represent a systematic extrapolation error (to the wall), a finite-size effect, or a measurable breakdown of the quasiexact nature of the Carnahan and Starling equation of state.
[28] Note that Fig. 9 of Ref. [8] actually plots twice what is stated in the caption.
[29] $\partial f/\partial\mu=-\partial^2 W/\partial\mu\partial h=\partial\langle N\rangle/\partial h$.
[30] R. Castaneda-Priego, A. Rodriguez-Lopez, and J. M. Mendez-Alcaraz, Phys. Rev. E **73**, 051404 (2006).
[31] J. A. Cuesta, Y. Martinez-Raton, and P. Tarazona, J. Phys.: Condens. Matter **14**, 11965 (2002).
[32] One might also be concerned that FMT-DFT is not fully consistent with the quasiexact surface equation of state (7). That this issue is almost certainly of minor significance can be seen from Fig. 1 of H. Hansen-Goos and R. Roth, J. Chem. Phys. **124**, 154506 (2006).
[33] L. J. Douglas Frink and A. G. Salinger, J. Chem. Phys. **110**, 5969 (1999).